Inorg. Chem. **2006**, *45*, 4372–4380

Synthesis and Characterization of a Tripodal Amide Ligand and Its Binding with Anions of Different Dimensionality

P. S. Lakshminarayanan, Eringathodi Suresh,* and Pradyut Ghosh*

Analytical Science Discipline, Central Salt & Marine Chemicals Research Institute (C.S.I.R.), G. B. Marg, Bhavnagar 364002, India

Received December 20, 2005

Synthesis and crystal structure of a tren-based amide, $\mathbf{L_1}$, *N*,*N*′,*N*′′-tris[(2-amino-ethyl)-3-nitro-benzamide] is reported. The crystallographic results show intramolecular hydrogen bonding and aromatic $\pi\cdots\pi$ stacking among tripodal arms which prevent opening of the receptor cavity. Intermolecular hydrogen bonding in $\mathbf{L_1}$ generates the sheetlike network in the solid state. The structural aspects of binding halides **(1** and **2)**, nitrate (**3**), perchlorate (**4**), and hexafluorosilicate (**5**) with the protonated $\mathbf{L_1}$ are examined crystallographically. Protonation at the apical nitrogen of $\mathbf{L_1}$ in the presence of anions shows a structural transformation from sheet to bilayer network. Anion binding with multiple receptor units is observed via amide N–H···anion and aryl C–H···anion hydrogen-bonding interactions in all the complexes. The aryl group having nitro functionality that contributes to anion binding in complexes **1**–**5** through CH···anion interactions (either para or meta to nitro C–H) is noteworthy. These studies also show higher anion coordination of chloride (8) and hexafluorosilicate (14) with $\mathbf{L_1}H^+$.

Introduction and Background

Anion complexation is a promising field in chemistry as coordination chemistry of anions has proven its roles in biological systems, in the environmental issues, and in the area of medicine and catalysis.[1,2] Recently, Bowman-James has categorized the binding of anions based on their coordination numbers similar to cation coordination originally developed by Werner.[3] Tris(2-aminoethyl)-amine, tren, is one of the important building blocks for the binding of halides, nitrate, phosphate, and sulfate which have been studied by different groups.[4−12] The binding ability of these tripodal receptors for anions varies with the attached moiety to the tren (N4) unit, since functional groups modify the hydrogen-bonding capability. Recent theoretical investigation by Hay et al. showed that the effect of electron withdrawing substituents on the aryl moiety significantly enhances the stability of anion complexes.[13] Anion receptors in nature often involve amide linkages as hydrogen-bond donors; hence, amide based ligands are important for anion binding study. In 1993 Reinhoudt and co-workers synthesized a new

* To whom correspondence should be addressed. E-mail: pradyut@csmcri.org. Fax: +91-278-2426970.

(1) (a) Bianchi, A., Bowman-James, K., García-España, E., Eds.; *Supramolecular Chemistry of Anions;* Wiley-VCH: New York, 1997. (b) Snellink-Ruel, B. H. M.; Antonisse, M. M. G.; Engbersen, J. F. J.; Timmerman, P.; Reinhoudt, D. N. *Eur. J. Org. Chem.* **2000**, 165. (c) Beer, P. D.; Gale, P. A. *Angew. Chem., Int. Ed.* **2001**, *40*, 486.

(2) (a) Best, M. D.; Tobey, S. L.; Anslyn, E. V. *Coord. Chem. Rev.* **2003**, *240*, 3. (b) McKee, V.; Nelson, J.; Town, R. M. *Chem. Soc. Rev.* **2003**, *32*, 309. (c) Sessler, J. L.; Camiolo, S.; Gale, P. A. *Coord. Chem. Rev.* **2003**, *240*, 17. (d) Llinares, J. M.; Powell, D.; Bowman-James, K. *Coord. Chem. Rev.* **2003**, *240*, 57. (e) Bondy, C. R.; Loeb, S. L. *Coord. Chem. Rev.* **2003**, *240*, 77. (f) Choi, K.; Hamilton, A. D. *Coord. Chem. Rev.* **2003**, *240*, 101. (g) Lambert, T. N.; Smith, B. D. *Coord. Chem. Rev.* **2003**, *240*, 143. (h) Davis, A. P.; Joos, J.-B. *Coord. Chem. Rev.* **2003**, *240*, 143. (i) Lee, C.-H.; Na, H.-K.; Yoon, D.-W.; Won, D.-H.; Cho, W.-S.; Lynch, V. M.; Shevchuk, S. V.; Sessler, J. L. *J. Am. Chem. Soc.* **2003**, *125*, 7301. (j) Wallace, K. J.; Belcher, W. J.; Turner, D. R.; Syed, K. F.; Steed, J. W. *J. Am. Chem. Soc.* **2003**, *125*, 9699.

(3) Bowman-James, K. *Acc. Chem. Res.* **2005**, *38*, 671.

(4) Valiyaveettil, S. K.; Engbersen, J. F. J.; Verboom, W.; Reinhoudt, D. N. *Angew. Chem., Int. Ed. Engl.* **1993**, *32*, 900.

(5) Beer, P. D.; Chen, Z.; Goulden, A. J.; Graydon, A.; Stokes, S. E.; Wear, T. *J. Chem. Soc., Chem. Commun.* **1993**, 1834.

(6) Beer, P. D.; Hopkins, P. K.; McKinney, J. D. *Chem. Commun.* **1999**, 1253.

(7) Tobey, S. L.; Jones, B. D.; Anslyn, E. V. *J. Am. Chem. Soc.* **2003**, *125*, 4026.

(8) Bazzicalupi, C.; Bencini, A.; Berni, E.; Bianchi, A.; Ciattini, S.; Giorgi, C.; Maoggi, S.; Paoletti, P.; Valtancoli, B. *J. Org. Chem.* **2002**, *67*, 9107.

(9) Kavallieratos, K.; Danby, A.; Van Berkel, G. J.; Kelly, M. A.; Sachleben, R. A.; Moyer, B. A.; Bowman-James, K. *Anal. Chem.* **2000**, *72*, 5258.

(10) Raposo, C.; Almaraz, M.; Martín, M.; Weinrich, V.; Mussóns, M. L.; Alcázar, V.; Caballero, M. C.; Morán, J. R. *Chem. Lett.* **1995**, *24*, 759.

(11) Hossain, M. A.; Liljegren, J. A.; Powell, D.; Bowman-James, K. *Inorg. Chem.* **2004**, *43*, 3751.

(12) Custelcean, R.; Moyer, B. A.; Hay, B. P. *Chem. Commun.* **2005**, 5971.

(13) Bryantsev, V. S.; Hay, B. P. *Org. Lett.* **2005**, *7*, 5031.

10.1021/ic052159o CCC: $33.50
Published on Web 04/26/2006

Chart 1. Tripodal Triamide Having Aryl Substitution $\mathbf{L_1}$, Tripodal Triamide Having Alkyl Substitution $\mathbf{L_2}$

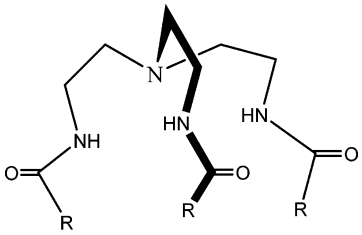

L_1: R = *m*-$C_6H_5NO_2$
L_2: R = -$(CH_2)_6CH_3$

series of tren-based tripodal ligands containing amide groups as anion receptors, where a conductivity study showed binding preference in the order $H_2PO_4^{2-} > Cl^- > HSO_4^-$.[4,14] In another study, Beer et al. have shown halide and ReO_4^- binding in the tripodal amide vicinity of the tren-based ligand by ^{1}H NMR titration.[15] In all these cases, anion binding by tripodal amide ligands is exclusively by hydrogen-bond formation. Structural information can provide insight on the proper binding topology of anions with these tripodal amide receptors. In this regard, Bowman-James et al. showed that the nitrate salt of a tripodal lipophilic amide $\mathbf{L_2}$ anion was not encapsulated in the cavity of a tren unit. This is simply because one of the amide carbonyl oxygen atoms points into the cavity to hydrogen-bond with the endo oriented part of the apical amine as observed from the structural investigation.[16] Given our interest in structural aspects of anion binding, we have extensively studied the coordination of a newly designed substituted tren-based triamide, $\mathbf{L_1}$, having nitro functionality with anionic guests of different shapes and geometry. Herein, we report structures of $\mathbf{L_1}$ (see Chart 1) and the binding of chloride, bromide (spherical), nitrate (trigonal planar), perchlorate (tetrahedral), and hexafluorosilicate (octahedral) with protonated $\mathbf{L_1}$ and their detailed molecular interactions.

Experimental Section

Materials. Tris(2-aminoethyl) amine and 3-nitrobenzoyl chloride were purchased from Aldrich chemicals and used as received. Hydrochloric acid, hydrobromic acid, nitric acid, and perchloric acid were received from SD Fine Chemicals, India, and hydrofluoric acid was received from Merck, India. All the solvents were purchased from SD Fine Chemicals, India, and were purified prior to use.

Synthesis. The tripodal amide $\mathbf{L_1}$ was synthesized by reacting tris(2-aminoethyl)amine (tren) with 3-nitrobenzoyl chloride at room temperature in a 1:3 molar ratio. The tren (0.146 g, 1 mmol) was dissolved with constant stirring at room temperature in 30 mL of dry tetrahydrofuran (THF) containing triethylamine (0.354 g, 3.5 mmol) to neutralize the acid formed during reaction. A solution of 3-nitrobenzoyl chloride (0.557 g, 3 mmol) in 50 mL of dry THF was added dropwise to the tren solution over a period of 1 h under dinitrogen atmosphere with constant stirring at room temperature. After the addition was complete, the reaction mixture was stirred for 24 h at room temperature, and the solution was filtered. Upon complete removal of the filtrate, the light yellow solid was washed three times with 100 mL of water and dried in air. Crystals suitable for X-ray diffraction were achieved by crystallization of the yellowish solid in DMSO. Complexes **1**, **2**, **3**, **4**, and **5** were obtained by dissolving $\mathbf{L_1}$ (50 mg) in 50 mL of MeOH/DMSO (2:3) and adding 1.5 equiv of 37% HCl, 49% HBr, HNO_3, 70% $HClO_4$, and 40% HF, respectively. The respective solutions were stirred at room temperature for 30 min and filtered in a 100 mL beaker. Filtrates were allowed to evaporate at room temperature, which yielded suitable crystals for X-ray analysis in 1 week.

L_1. Yield: 75%, mp 210 °C. ^{1}H NMR (200 MHz, DMSO-d_6): δ 3.605−3.829 (m, 12H, NCH_2CH_2), 7.67−8.56 (m, 12H, Ar*H*), 9.386 (br, 3H, −NH). ^{13}C NMR (50 MHz, DMSO-d_6): δ 35.40 (NCH_2), 53.02 (NCH_2CH_2), 123.18, 126.99, 130.99, 134.70, 136.03, and 148.68 (Ar), 165.94 (C═O). MS (ESI): *m*/*z* 594.2 [**L**]$^+$. Anal. Calcd for $C_{27}H_{27}N_7O_9$: C, 54.64; H, 4.58; N,16.51. Found: C, 54.75; H, 4.52; N, 16.43.

$L_1H^+\cdot Cl^-$, 1. Yield: 65%, mp > 250 °C. ^{1}H NMR (200 MHz, DMSO-d_6): δ 3.598−3.804 (m, 12H, NCH_2CH_2), 7.66−8.55 (m, 12H, Ar*H*), 9.326 (br, 3H, −NH). ^{13}C NMR (50 MHz, DMSO-d_6): δ 34.26 (NCH_2), 52.72 (NCH_2CH_2), 121.99, 125.93, 129.93, 133.58, 134.9, and 147.58 (Ar), 164.90 (C═O). MS (ESI): *m*/*z* 594.16 [**L**]$^+$. Anal. Calcd for $C_{27}H_{28}$ Cl N_7 O_9: C, 51.47; H, 4.48; N, 15.56. Found: C, 51.04; H, 4.35; N, 15.64.

$L_1H^+\cdot Br^-$, 2. Yield: 60%, mp > 250 °C. ^{1}H NMR (200 MHz, DMSO-d_6): δ 3.622−3.766 (m, 12H, NCH_2CH_2), 7.67−8.51 (m, 12H, Ar*H*), 9.19 (br, 3H, −NH). ^{13}C NMR (50 MHz, DMSO-d_6): δ 34.41 (NCH_2), 52.24 (NCH_2CH_2), 122.31, 126.25, 130.50, 134.16, 135.19, and 147.63 (Ar), 165.41 (C═O). MS (ESI): *m*/*z* 594.5 [**L**]$^+$. Anal. Calcd for $C_{27}H_{28}$ Br N_7 O_9: C,48.08; H, 4.18; N, 14.53. Found: C, 47.85; H, 4.08; N, 14.64.

$L_1H^+\cdot NO_3^-$, 3. Yield: 45%, mp > 250 °C. ^{1}H NMR (200 MHz, DMSO-d_6): δ 3.587−3.796 (m, 12H, NCH_2CH_2), 7.65−8.51 (m, 12H, Ar*H*), 9.276 (br, 3H, −NH). ^{13}C NMR (50 MHz, DMSO-d_6): δ 33.94 (NCH_2), 51.20 (NCH_2CH_2), 122.99, 126.44, 130.24, 134.04, 137.10, and 148.48 (Ar), 166.00 (C═O). MS (ESI): *m*/*z* 594.16 [**L**]$^+$. Anal. Calcd for $C_{27}H_{28}N_8$ O_{12}: C, 49.39; H, 4.30; N, 17.06. Found: C, 49.52; H, 4.40; N,17.01.

$L_1H^+\cdot ClO_4^-$, 4. Yield: 40%, mp > 250 °C. ^{1}H NMR (200 MHz, DMSO-d_6): δ 3.541−3.83 (m, 12H, NCH_2CH_2), 7.662−8.533 (m, 12H, Ar*H*), 9.378 (br, 3H, −NH). ^{13}C NMR (50 MHz): ^{13}C NMR (50 MHz, DMSO-d_6): δ 34.60 (NCH_2), 52.16 (NCH_2CH_2), 122.35, 125.88, 130.19, 133.74, 135.07, and 148.03 (Ar), 164.90 (C═O). MS (ESI): *m*/*z* 594.16 [**L**]$^+$. Anal. Calcd for $C_{27}H_{28}Cl_8N_7O_{13}$: C, 46.72; H, 4.06; N, 14.12. Found: C, 46.42; H, 4.14; N, 14.22.

$L_1H^+\cdot 0.5SiF_6\cdot 0.5H_2O$, 5. Yield: 60%, mp > 250 °C. ^{1}H NMR (200 MHz, DMSO-d_6): δ 3.50−3.69 (br, 12H, NCH_2CH_2), 7.65−8.53 (m, 12H, Ar*H*), 9.026 (br, 3H, −NH). ^{13}C NMR (50 MHz, DMSO-d_6): δ 34.20 (NCH_2), 52.51 (NCH_2CH_2), 121.79, 125.78, 129.90, 133.40, 138.91, and 147.56 (Ar). MS (ESI): *m*/*z* 594.2 [**L**]$^+$. Anal. Calcd for $C_{27}H_{29}$ F_3N_7 $O_{9.5}$ $Si_{0.5}$: C, 48.07; H, 4.33; N, 14.53. Found: C, 47.68; H, 4.18; N,14.42.

Physical Measurements. ^{1}H and ^{13}C NMR spectra were recorded on a Bruker 200 spectrometer and a 50 MHz FT-NMR spectrometer (model: Avance-DPX200), respectively. Elemental data were recorded on a Perkin-Elmer 4100 elemental analyzer. MS (ESI) measurements were carried out on Waters QTof-Micro instruments.

X-ray Crystallography. The crystallographic data and details of data collection for $\mathbf{L_1}$ and **1**−**5** are given in Table 1. In each case, a crystal of suitable size was selected from the mother liquor

(14) Potvin and Jairam also have used similar types of ligands for binding metal ions. Jairam, R.; Potvin, P. G. *J. Org. Chem.* **1992**, *57*, 4136.
(15) Beer, P. D.; Hopkins, P. K.; McKinney, J. D. *Chem. Commun.* **1999**, 1253.
(16) Danby, A.; Seib, L.; Bowman-James, K.; Alcock, N. W. *Chem. Commun.* **2000**, 973.

Table 1. Crystallographic Data for $\mathbf{L_1}$, $\mathbf{L_1}H^+\cdot Cl^-$ (**1**), $\mathbf{L_1}H^+\cdot Br^-$ (**2**), $\mathbf{L_1}H^+\cdot NO_3^-$ (**3**), $\mathbf{L_1}H^+\cdot ClO_4^-$ (**4**), and $\mathbf{L_1}H^+\cdot 0.5SiF_6\cdot 0.5H_2O$ (**5**)

	$\mathbf{L_1}$	**1**	**2**	**3**	**4**	**5**
empirical formula	$C_{27}H_{27}N_7O_9$	$C_{27}H_{28}ClN_7O_9$	$C_{27}H_{28}BrN_7O_9$	$C_{27}H_{28}N_8O_{12}$	$C_{27}H_{28}ClN_7O_{13}$	$C_{27}H_{29}F_3N_7O_{9.5}Si_{0.5}$
fw	593.56	630.01	674.47	656.57	694.01	674.62
cryst syst	monoclinic	monoclinic	triclinic	triclinic	triclinic	monoclinic
space group	$P21/c$	$P21/n$	$P\bar{1}$	$P\bar{1}$	$P\bar{1}$	$C2/c$
a (Å)	12.3801(10)	11.2216(11)	8.6030(8)	8.9077(7)	8.4898(9)	32.360(2)
b (Å)	8.4898(9)	11.5117(11)	11.3256(11)	11.3308(10)	11.3902(11)	11.8115(8)
c (Å)	26.698(2)	21.550(2)	15.6270(15)	15.5060(13)	16.0933(16)	15.2928(10)
α (deg)	90.00	90.00	69.9320(10)	71.7490(10)	73.175(2)	90.00
β (deg)	90.969(2)	83.523(2)	80.784(2)	84.043(2)	93.1220(10)	
γ (deg)	90.00	90.00	76.401(2)	74.304(2)	78.113(2)	90.00
V (Å^3)	2721.0(4)	2783.4(5)	1389.2(2)	1426.0(2)	1456.0(3)	5836.5(7)
Z	4	4	2	2	2	8
d_{calcd} (g/cm^3)	1.449	1.503	1.612	1.529	1.583	1.535
cryst size (mm^3)	0.32 × 0.25 × 0.10	0.20 × 0.10 × 0.07	0.43 × 0.32 × 0.28	0.31 × 0.25 × 0.22	0.46 × 0.38 × 0.26	0.26 × 0.14 × 0.12
F(000)	1240	1312	692	684	720	2800
μ Mo Kα (mm^{-1})	0.111	0.206	1.549	0.123	0.215	0.149
T (K)	100(2)	100(2)	100(2)	100(2)	100(2)	100(2)
θ range	1.55−28.26	1.89−28.29	1.39−28.31	1.39−28.24	1.32−28.27	1.26−28.28
reflns collected	15 371	16 272	11 782	8448	8658	16 965
independent reflns	6252	6445	6238	6236	6366	6784
R(int)	0.0237	0.0610	0.0285	0.0154	0.0195	0.0342
data/restraints/params	6252/0/400	6445/0/413	6238/0/406	6236/0/440	6366/0/476	6784/0/445
R1; wR2	0.0453; 0.1174	0.0637; 0.1214	0.0435; 0.1046	0.0461; 0.1164	0.0537; 0.1329	0.0499; 0.1177
GOF (F^2)	1.064	1.022	1.095	1.070	1.060	1.075

and immersed in partone oil, and then it was mounted on the tip of a glass fiber and cemented using epoxy resin. Intensity data for all crystals were collected using Mo Kα (λ = 0.7107 Å) radiation on a Bruker SMART APEX diffractometer equipped with a CCD area detector at 100 K. The data integration and reduction were processed with SAINT[17a] software. An empirical absorption correction was applied to the collected reflections with SADABS[17b] using XPREP.[17a] The structures were solved by direct methods using SHELXTL[18] and were refined on F^2 by the full-matrix least-squares technique using the SHELXL-97[19] program package. Graphics are generated using PLATON[20] and MERCURY 1.3.[21] In all the six compounds, non-hydrogen atoms were refined anisotropically. Hydrogen atoms attached to all carbon atoms were geometrically fixed while the hydrogen atoms of amide, tertiary amino nitrogen of the salts, were located from the difference Fourier map, and the positional and temperature factors are refined isotropically.

Results and Discussion

Synthesis. The acyclic tripodal derivative ligand $\mathbf{L_1}$ has been synthesized, and the single-crystal investigation has been carried out in an attempt to understand the binding capacity of this ligand with different anions. The synthesis of $\mathbf{L_1}$ is straightforward and involves a simple acid chloride reaction of the amine tren with 3 equiv of 3-nitrobenzoyl chloride. Crystallization is accomplished in DMSO with high yield. Complexes **1**−**5** were obtained by titrating $\mathbf{L_1}$ with respective acids in a methanol/DMSO binary solvent, and crystallization was obtained by slow evaporation. Syntheses of these salts were also straightforward, resulting in high yields.

Crystallographic Studies. $\mathbf{L_1}$. The neutral triamide ligand $\mathbf{L_1}$ crystallizes in monoclinic space group $P2_1/c$ (Table 1), and the ORTEP diagram of the ligand moiety with atom numbering scheme is depicted in Figure 1a. The same atom numbering for the ligand is retained in all the structures **1**−**5** presented in this investigation.[22] The crystal structure of $\mathbf{L_1}$ shows strong intramolecular hydrogen-bonding interactions between two arms of the tripodal ligand. Amide oxygen O4 of one arm acts as an acceptor and is involved in N−H···O and C−H···O interactions with the donor amide hydrogen H2N and phenyl hydrogen H9 from the other arm (N2···O4 = 2.816 Å, ∠N2−H2N···O4 = 175.4°; C9···O4 = 3.169 Å, ∠C9−H9···O4 = 164°).[23] These intramolecular hydrogen bondings assist the phenyl ring (C13−C18) to be in closer proximity to the phenyl ring (C22−C27) of the third arm which is not involved in any intramolecular hydrogen bonding. The distance between the centroids of the π-stacked phenyl rings (C1g and C2g) is 3.754 Å (Figure 1b).[24] The

(17) (a) Sheldrick, G. M. *SAINT and XPREP*, version 5.1; Siemens Industrial Automation Inc.: Madison, WI, 1995. (b) *SADABS, Empirical Absorption Correction Program;* University of Göttingen: Göttingen, Germany, 1997.
(18) Sheldrick, G. M. *SHELXTL Reference Manual*, version 5.1; Bruker AXS: Madison, WI, 1997.
(19) Sheldrick, G. M. *SHELXL-97: Program for Crystal Structure Refinement;* University of Göttingen: Göttingen, Germany, 1997.
(20) Spek, A. L. *PLATON-97;* University of Utrecht: Utrecht, The Netherlands, 1997.
(21) *Mercury 1.3 Supplied with Cambridge Structural Database;* CCDC: Cambridge, U.K., 2003−2004.
(22) See Supporting Information.
(23) For some representative examples of C−H···O interaction, see the following: (a) Desiraju, G. R. *Chem. Commun.* **2005**, 2995. (b) Steiner, T. *Angew. Chem., Int. Ed.* **2002**, *41*, 48. (c) Desiraju, G. R.; Steiner, T. *The Weak Hydrogen Bond in Structural Chemistry and Biology;* Oxford University Press: Oxford, U.K., 1999. (d) Desiraju, G. R. *Angew. Chem., Int. Ed. Engl.* **1995**, *34*, 2311. (e) Thallapally, P. K.; Katz, A. K.; Carrell, H. L.; Desiraju, G. R. *CrystEngComm* **2003**, *5*, 87.
(24) (a) Kaafarani, B. R.; Wex, B.; Olover, A. G.; Bauer, J. A. K.; Neckers, D. C. *Acta Crystallogr.* **2003**, *E59*, o227. (b) Garden, S. J.; da Cunha, F. R.; Wardell, J. L.; Skakle, J. M. S.; Low, J. N.; Glidewell, C. *Acta Crystallogr.* **2002**, *C58*, o463.

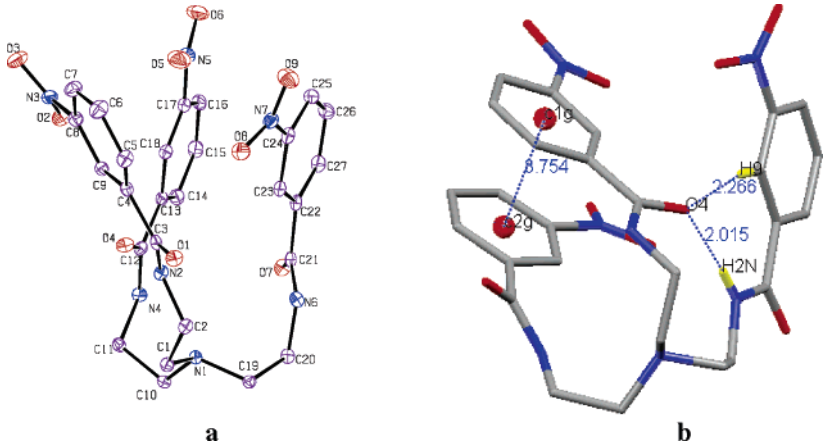

Figure 1. (a) ORTEP drawing of $\mathbf{L_1}$ with atom numbering scheme; (b) $\mathbf{L_1}$ showing N−H···O, aryl C−H···O, and aromatic $\pi\cdots\pi$ interactions (distances are in Å).

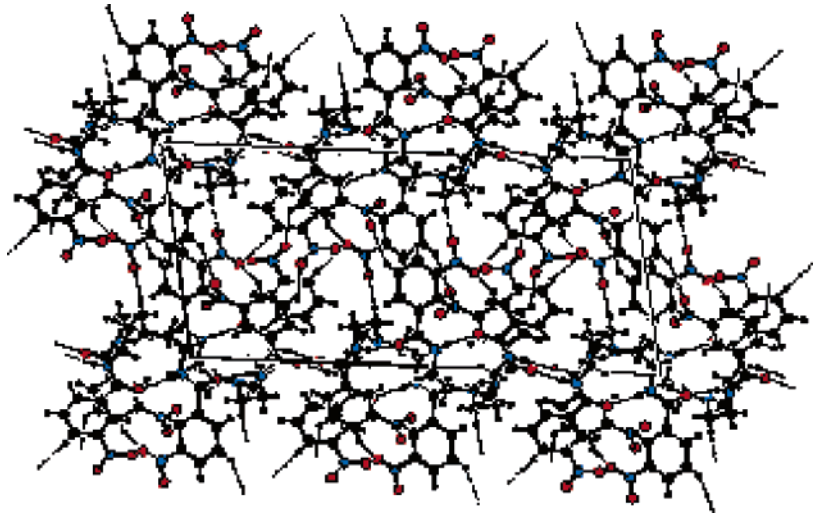

Figure 2. Packing diagram of $\mathbf{L_1}$ viewed down the *b*-axis with various hydrogen-bonding interactions showing 2D-sheet architecture along the *ac*-plane.

combined effect of intramolecular hydrogen bonding and aromatic $\pi\cdots\pi$ stacking is to resist the opening of the tripodal amide ligand. The torsion angles involving $N1_{apical}CCN_{amide}$ are in folded conformation with angles 80.97, 63.10, and 64.49° for three arms composed of the amide nitrogen N2, N4, and N6, respectively, whereas torsion angles involving the carbon atoms connecting the terminal phenyl rings in each arm are almost in extended conformation with angles 174.88°, −179.11°, and 173.70°, respectively.

The packing diagram of the molecule showing various intermolecular hydrogen-bonding interactions (Supporting Information, Table 1S) as viewed down the *b*-axis is depicted in Figure 2. Ligand moieties are oriented in the opposite direction with a strong dimeric association via the N−H···O interaction. The amide nitrogen N6 is involved in N−H···O intermolecular hydrogen bonding with the amide oxygen O1 (N6···O1 = 2.820 Å, ∠N6−H6N···O1 = 164(2)°). Associated dimers are further involved in N−H···O interactions from either end (N4···O7 = 2.823 Å, ∠N4−H4···O7 = 151.82°) extending a one-dimensional layered arrangement of molecules along the *c*-axis. These one-dimensional dimers are further cross-linked via the C−H···O interaction between the nitro oxygen atoms which are oriented on either side of the associated dimers creating a two-dimensional hydrogen-bonded sheetlike arrangement (Figure 2). The nitro oxygens (O2, O3, O6, and O9) act as acceptors in C−H···O intermolecular hydrogen bonding with C···O distances and C−H···O angles ranging from 3.216 to 3.492 Å and from 125 to 172°, respectively.

$\mathbf{L_1H^+\cdot Cl^-}$, 1. The compound **1** crystallizes in monoclinic space group $P2_1/n$ (Table 1), and the tertiary nitrogen of the tripodal ligand is protonated and turns out to be the monochloride salt of the amide ligand. The endo oriented proton H1 of the apical amine is in trifurcated N−H···O intramolecular hydrogen bonding with the three amide oxygens of the receptor arms without encapsulation of chloride within the tren unit. The packing diagram of complex **1** viewed down the *b*-axis (Figure 3) shows that the cationic array of the ligands is arranged diagonal to the *ac*-plane with chloride between the adjacent bilayers. The ligand moieties are organized via intermolecular C−H···O interactions between the alkyl hydrogen from all three arms of the $\mathbf{L_1}$ with one oxygen from each nitro group. Details of various hydrogen-bonding interactions with the symmetry code is given in the hydrogen-bonding table (Supporting Information, Table 2S). The binding of chloride by pronon-ated $\mathbf{L_1}$ is shown in Figure 4.

It clearly shows that the one chloride is surrounded by

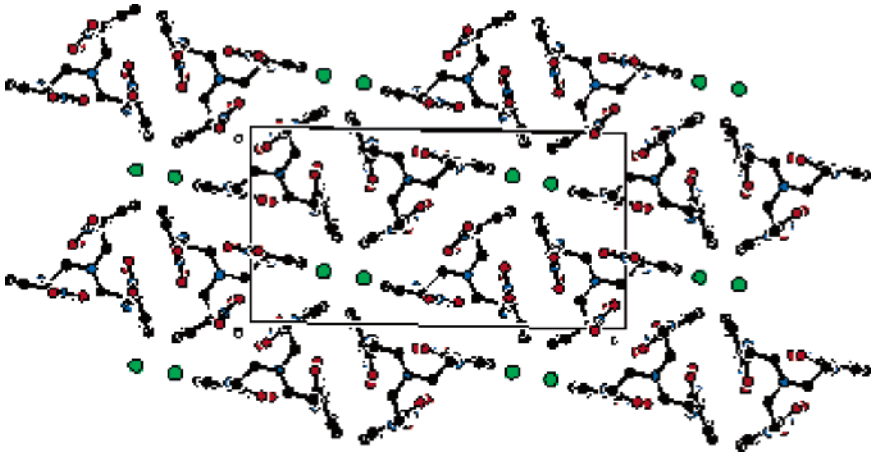

Figure 3. PLATON packing viewed down the *b*-axis showing the arrangement of the cationic $\mathbf{L_1}$ almost diagonal to the *ac*-plane with the chloride anion situated between the adjacent cationic arrays (color code: Cl, green; N, blue; C, black; O, red).

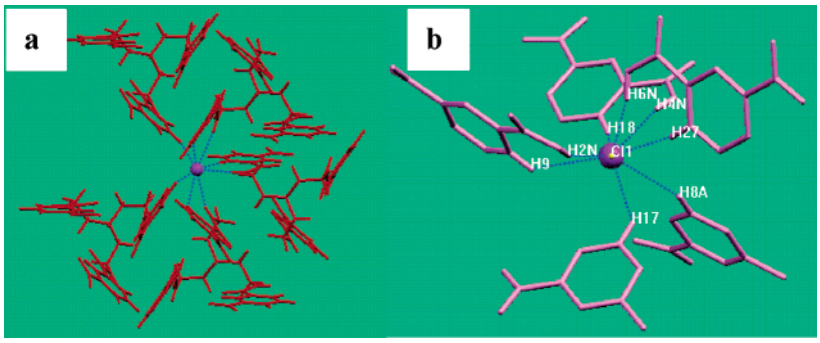

Figure 4. (a) MERCURY diagram depicting the interactions of the chloride (pink with dotted blue hydrogen bonding) with the $\mathbf{L_1}H^+$; (b) close-up view of eight hydrogen-bonding interactions with chloride and close-up view of chloride binding.

five $\mathbf{L_1}$ moieties having eight hydrogen-bonding contacts (Figure 4a and Table 2). These are three N−H···Cl^- interactions of the amide nitrogen atoms, N2, N4, and N6 of different $\mathbf{L_1}$ units, and five contacts via C−H···Cl^- interactions from the meta and para hydrogens with respect to the nitro group of the phenyl ring (Figure 4b and Table 2). Higher coordination (7 or 8) is observerd in larger or multiatomic anion-like sulfate and nitrate etc., whereas chloride generally prefers hexacoordination.[3,25] An unusual octacoordination in chloride complex **1** may be because of the possibility of the closer approach by multiple ligand units toward the anion to attain a stable bilayer arrangement in the solid state. The N···Cl^- distances range from 3.169 to 3.473 Å with N−H···Cl^- angles ranging from 156 to 166°, which is in good agreement with the reported values.[25a,26] H8A (meta) and H9 (para) with respect to nitro of aryl moiety interact with the chloride with C···Cl^- distances of 3.461 and 3.448 Å and C−H···Cl^- angles of 141 and 134°, respectively, whereas H17 (meta) and H18 (para) form C···Cl^- distances of 3.489 and 3.492 Å and C−H···Cl angles of 137 and 154°, respectively. Further, para hydrogen H27 completes the last contact with the anion having a C···Cl^- distance of 3.664 Å and a C−H···Cl^- angle of 171° which are all in good agreement with the C−H···Cl^- contact reported experimentally and theoretically.[13,25a,27] Thus, the eight-point contact via N−H···Cl^- and C−H···Cl^- interactions is responsible for the binding of the chloride ion with the protonated $\mathbf{L_1}$ receptor outside the tren cavity. In the case of the solution-state study by ^{1}H NMR, when HCl was added to the DMSO-d_6 solution of $\mathbf{L_1}$, the ^{1}H NMR spectrum shows a shift in the position of the tren NCH_2 proton from δ 3.678 ppm to the higher δ value of 3.844 ppm. This shift indicates the influence of the protonated apical nitrogen on the neighboring proton. Moreover, spectral changes also observed in the aromatic regions support the anion binding with $\mathbf{L_1}H^+$ in solution state.[22]

$\mathbf{L_1}H^+\cdot Br^-$, 2. The solid-state structure of complex **2** (Table 1) shows intramolecular N−H···O interaction between the hydrogen of the protonated tertiary nitrogen with the amide oxygen O4 (N(1)···O(4) = 2.764(3) Å, ∠N(1)−H(1N)···O(4) = 158°) and the amide hydrogen H(2N) with O7 of the other arm (N2···O7 = 2.946(4) Å, ∠N(2)−H(2N)···O(7) = 152(4)°), restricting the size of the tren cavity toward the encapsulation of bromide. The packing diagram viewed down the *a*-axis (Figure 5) along with the hydrogen-bonding interactions clearly shows that the receptor packs in a bilayer array with the bromide between the adjacent bilayers. Intermolecular C−H···O hydrogen bonding between alkyl hydrogen H10A and nitro oxygen O5 is bridging the receptor

(25) (a) Ilioudis, C. A.; Tocher, D. A.; Steed, J. W. *J. Am. Chem. Soc.* **2004**, *126*, 12395. (b) Lakshminarayanan, P. S.; Kumar, D. K.; Ghosh, P. *Inorg. Chem.* **2005**, *44*, 7540.
(26) Kang, S. O.; Llinares, J. M.; Powell, D.; VanderVelde, D.; Bowman-James, K. *J. Am. Chem. Soc.* **2003**, *125*, 10152.
(27) (a) Chmielewski, M. J.; Charon, M.; Jurczak, J. *Org. Lett.* **2004**, *6*, 3501. (b) Bryantsev, V. S.; Hay, B. P. *J. Am. Chem. Soc.* **2005**, *127*, 8282.

Table 2. Hydrogen Bonding Interactions between Anions and L_1H^+ in Complexes **1**−**5**

complex	D−H···A[a]	*d*(H···A) (Å)	*D*(D···A) (Å)	∠DHA (deg)
$L_1H^+ \cdot Cl^-$, **1**	N(2)−H(2N)···Cl(1)[1]	2.48(3)	3.285(2)	160(3)
	N(4)−H(4N)···Cl(1)[2]	2.71(2)	3.473(2)	166(2)
	N(6)−H(6N)···Cl(1)[3]	2.34(3)	3.169(2)	156(2)
	C(8)−H(8A)···Cl(1)[4]	2.69	3.461(3)	141
	C(9)−H(9)···Cl(1)[1]	2.78	3.488(2)	134
	C(17)−H(17)···Cl(1)[5]	2.75	3.489(3)	137
	C(18)−H(18)···Cl(1)[2]	2.64	3.492(2)	154
	C(27)−H(27)···Cl(1)[3]	2.74	3.664(2)	171
$L_1H^+ \cdot Br^-$, **2**	N(4)−H(4N)···Br(1)[1]	2.56	3.397(3)	158
	N(6)−H(6N)···Br(1)[2]	2.64(4)	3.363(3)	154(4)
	C(18)−H(18)···Br(1)[1]	2.84	3.765(3)	176
$L_1H^+ \cdot NO_3^-$, **3**	N(2)−H(2N)···O(10)[1]	1.95(3)	2.869(2)	168(2)
	N(4)−H(4N)···O(10)[2]	2.16(3)	2.910(2)	160(2)
	C(10)−H(10B)···O(11)[3]	2.55	3.252(3)	129
	C(17)−H(17)···O(10)[4]	2.55	3.454(2)	164
	C(18)−H(18)···O(10)[2]	2.45	3.335(2)	159
$L_1H^+ \cdot ClO_4^-$, **4**	N(4)−H(4N)···O(12)[1]	2.29(3)	2.988(4)	142(3)
	N(6)−H(6N)···O(13)[3]	2.25(3)	3.110(6)	173(3)
	C(10)−H(10A)···O(10)[4]	2.55	3.146(4)	119
	C(17)−H(17)···O(13)[2]	2.57	3.442(5)	157
	C(26)−H(26)···O(12)[5]	2.52	3.208(5)	131
	C(27)−H(27)···O(13)[3]	2.15	3.073(6)	172
$L_1H^+ \cdot 0.5SiF_6 \cdot 0.5H_2O$, **5**	O(1W)−H(1O)···F(1)[1]	2.13(4)	2.827(3)	138(3)
	N(2)−H(2N)···F(3)[2]	2.08(2)	2.819(2)	157(2)
	N(2)−H(2N)···F(2)[3]	2.48(2)	2.849(2)	110(1)
	N(6)−H(6N)···F(2)[1]	1.91(2)	2.7623(19)	173.6(19)
	C(2)−H(2A)···F(1)[2]	2.39	3.284(2)	152
	C(2)−H(2B)···F(3)[1]	2.29	3.231(2)	163

[a] Symmetry codes. Complex **1**: (1) $-x, 1-y, 1-z$; (2) $1-x, 1-y, 1-z$; (3) $x, y, 1+z$ (4) $-1/2+x, 3/2-y, 1/2+z$; (5) $1/2+x, 3/2-y, 1/2+z$. Complex **2**: (1) $x, -1+y, z$; (2) $1+x, -1+y, z$. Complex **3**: (1) $-x, 1-y, 1-z$; (2) $1-x, 1-y, 1-z$; (3) $x, 1+y, -1+z$; (4) $1+x, y, -1+z$. Complex **4**: (1) $-x, 1-y, 1-z$; (2) $x, y, -1+z$; (3) $1-x, 1-y, 1-z$; (4) $x, 1+y, -1+z$; (5) $1+x, y, -1+z$. Complex **5**: (1) x, y, z; (2) $1-x, -y, -z$; (3) $x, -y, -1/2+z$.

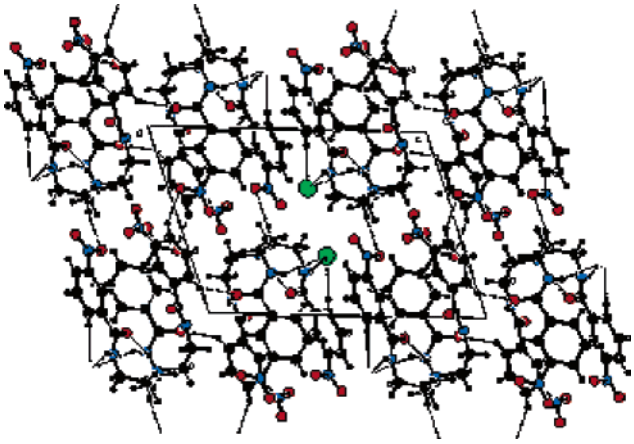

Figure 5. PLATON packing diagram with hydrogen-bonding interactions viewed down the *a*-axis for **2** (color code: Br, green; N, blue; C, black; aO, red).

moieties along the *b*-axis (C10···O5 = 3.405 Å, ∠C10−H10A···O5 = 153°) (Supporting Information, Table 3S). The adjacent monolayers of the ligand array are further connected via C−H···O hydrogen-bonding interactions involving the phenyl hydrogens H9A and H7 with the amide and nitro oxygens O7 and O9, respectively (C7···O9 = 3.407(4) Å, ∠C7−H7A···O9 = 155°; C9···O7 = 3.226(4) Å, ∠C9−H9A···O7 = 148°), forming the bilayers along the *c*-axis, whereas bilayers are oriented diagonal to the *ac*-plane in the case of complex **1**.

The binding of bromide with the receptor is depicted in Figure 6a, which shows that bromide is in a hydrogen-bonding interaction with two L_1H^+ via two N−H···Br^- contacts and one C−H···Br^- contact compared to eight-point contacts in the case of chloride complex **1**. The close-up view of the hydrogen-bonding pattern with the bromide guest is shown in Figure 6b, and the contact distances and angles with symmetry codes are given in Table 2. Amide hydrogens H6 and H18 (para with respect to the nitro group) make N−H···Br^- and C−H···Br^- interactions (N4···Br(1) = 3.397(3) Å, ∠N(4)−H(4N)···Br(1) = 158°; C(18)···Br(1) = 3.765(3) Å, ∠C(18)−H(18)···Br(1) = 176°), whereas the third N−H···Br^- interaction (N(6)···Br(1) = 3.363(3), ∠N(6)−H(6N)···Br(1) = 154(4)°) is formed from the amide hydrogen H6N of the other ligand making effective three-point contacts for the anion binding. The hydrogen bond distances and angles for N−H···Br^- and C−H···Br^- are within the normal range.[25]

$L_1H^+ \cdot NO_3^-$, 3. Compound **3**, mononitrate salt of the amide L_1, monoprotonated at the apical nitrogen, crystallizes in triclinic space group $P\bar{1}$, having two intramolecular N−H···O interactions (N(1)···O(4) = 2.757(2), ∠N(1)−H(1N)···O(4) = 156(2)°; N(6)···O(1) = 2.929(2) Å, ∠N(6)−H(6N)···O(1) = 151(2)°) as observed in the case of **2**. The receptor also packs bilayers of similar fashion of the ligand moieties as observed in complex **2** (Supporting Information, Table 4S). The nitrate guest is intercalated between the bilayers by a five-point attachment provided by four triamide receptor units (Figure 7a). A close-up view of the nitrate binding making various contacts is depicted in Figure 7b with relevant contact distances and angles given in Table 2. Recently, Steed et al. has also reported a simple pyridyl ligand containing a urea derivative templated by nitrate via

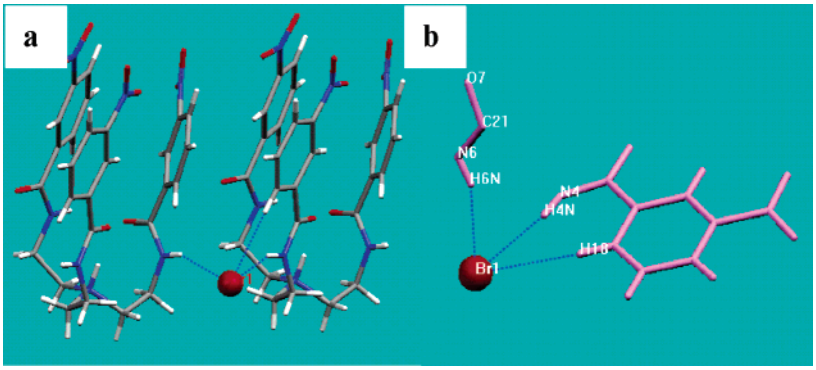

Figure 6. (a) MERCURY diagram depicting the hydrogen-bonding interaction (dotted blue line) between the bromide anion (red ball) with the cationic tripodal ligand; (b) close-up view of bromide binding.

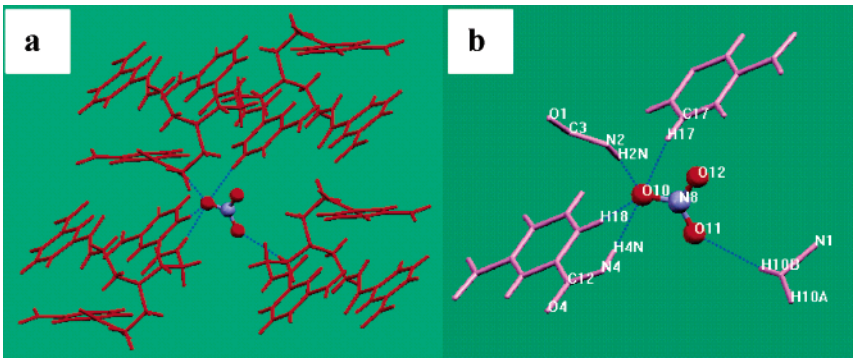

Figure 7. (a) MERCURY diagram depicting the hydrogen-bonding interaction (dotted blue line) between the nitrate with four protonated surrounding tripodal ligand moieties; (b) close-up view of nitrate binding.

a five-point N−H···O and C−H···O contact.[28] In complex **3**, O10 of the nitrate is involved in four contacts: two N−H···O interactions with amide hydrogens H2N and H4N (N(2)···O(10) = 2.869(2) Å, ∠N(2)−H(2N)···O(10) = 168(2)°; N(4)···O(10) = 2.910(2) Å, ∠N4−H(4N)···O(10) = 160-(2)°) and two C−H···O interactions with the phenyl hydrogens H17 (meta) and H18 (para) (C(17)···O(10) = 3.454(2) Å, ∠C(17)−H(17)···O(10) = 164°; C(18)···O(10) = 3.335 Å, ∠C(18)−H(18)···O(10) = 159°).

In addition to the above four interactions, O11 is in weak C−H···O contact with the methylene hydrogen H10B (C(10)···O(11) = 3.252(3) Å, ∠C(10)−H(10B)···O(11) = 129°), completing the fifth contact to stabilize the nitrate in the receptor channel.[27b,28] In contrast, the theoretical investigation by Hay et al. on the nitrate complex of $\mathbf{L_1}$ shows a 1:1 complex formation between $\mathbf{L_1}$ and NO_3^- via three N−H···O and three aryl C−H···O interactions making six-point contacts.[13]

$L_1H^+ \cdot ClO_4^-$, 4. In complex **4**, similar intramolecular N−H···O hydrogen bonding exists as observed in **2** and **3**, and details of these interactions with symmetry codes are given in Table 5S. Three oxygen atoms in perchlorate are disordered at two positions with occupancies of 0.6 and 0.4, respectively. As observed in complexes **2** and **3**, a similar bilayer arrangement of the ligand moiety is retained via various C−H···O and N−H···O interactions in the packing diagram of **4** (Table 5S). Perchlorate anions are entrapped between the neighboring bilayers via C−H···O and N−H···O contacts. Each perchlorate ion is encircled by five cationic ligands having six contacts (Figure 8a and Table 2). A close-up view of perchlorate binding with the receptor is shown in Figure 8b for clarity. O12 of the perchlorate ion is making one N−H···O (amide hydrogen H4N) interaction and one C−H···O (meta hydrogen H26) interaction, whereas O13 is in contact with the amide hydrogen H6N (N−H···O) and makes two C−H···O interactions with aryl hydrogen H17 (meta) and H27 (para). Perchlorate oxygen O10 (with no disorder) is forming a weak C−H···O contact with the methylene hydrogen H10A stabilizing the perchlorate guest.

$L_1H^+ \cdot 0.5SiF_6^{2-} \cdot 0.5H_2O$, 5. Silicon hexafluoride salt **5** was obtained on reaction of the tripodal ligand $\mathbf{L_1}$ with HF, presumably as a result of glass corrosion. The structure of the salt is a protonated tripodal cation with SiF_6^{2-} and half a water molecule (O1w) as solvent of crystallization. Both the SiF_6^{2-} and the water molecule (O1w) possess 2-fold symmetry passing through Si and O, respectively. Complex **5** retained the similar N−H···O intramolecular hydrogen-bonding pattern observed in previous cases (Table 6S). The receptor in complex **5** packs beautifully into the bilayer structure like other complexes via the effective intermolecular C−H···O interaction between the nitro oxygens (O3, O8, and O9) and the alkyl/aryl hydrogens (H1A, H10B, and H18), whereas amide oxygen O7 makes contact with aryl hydrogen H16.[22] SiF_6^{2-} and the lattice water molecule are positioned in the available space between the adjacent bilayers by various hydrogen-bonding modes.

In an attempt to understand the polyatomic anion (SiF_6^{2-})

(28) Turner, D. R.; Spencer, E. C.; Howard, J. A. K.; Tocher, D. A.; Steed, J. W. *Chem. Commun.* **2004**, 1352.

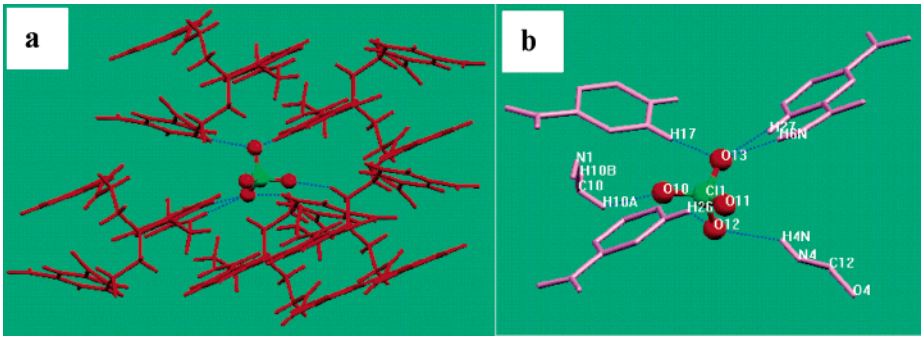

Figure 8. (a) MERCURY diagram depicting the perchlorate binding via C−H···O and N−H···O interactions with five $\mathbf{L_1}H^+$ moieties (in the case of O12 and O13, disorder positions which are in contact with the ligand are shown for clarity); (b) close-up view of perchlorate binding.

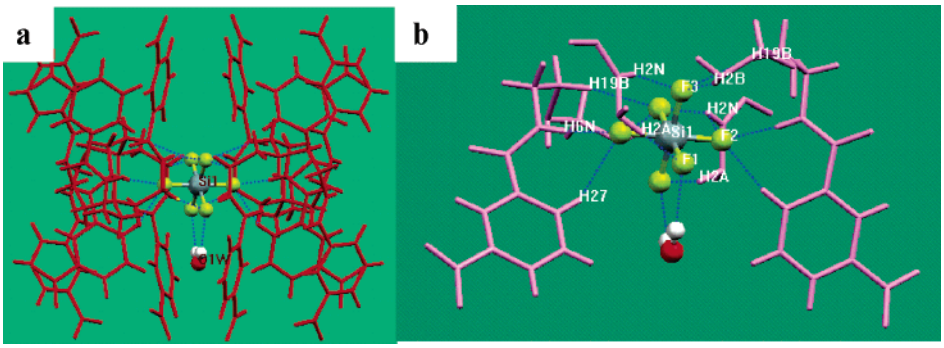

Figure 9. MERCURY diagram showing the various molecular interactions (dotted blue line) of the hexaflurosilicate from four surrounding tripodal anions and one lattice water molecule; (b) close-up view of hexafluorosilicate binding.

binding by the tripodal amide $\mathbf{L_1}H^+$, we have analyzed the interaction of SiF_6^{2-} with the surrounding ligand moieties and lattice water (Figure 9).

The fluoride atoms (F1 and F2) of SiF_6^{2-} are each making two contacts, whereas F3 is making three contacts with the surrounding receptor moieties and water molecule resulting in 14 hydrogen-bonding contacts on SiF_6^{2-}. F1 is involved in the C−H···F interaction with H2A of the methylene hydrogen (C2−H2A···F1; C(2)···F(1) = 3.284(2) Å; ∠C2−H2···F1 = 152°), whereas the second contact is provided by the water molecule forming O−H···F hydrogen bonding (O1w−H(1O)···F = 2.827(3) Å and angle ∠O1w−H(1O)···F(1) = 138(3)°). F2 is involved in one strong and another weak NH···F contact with the amide hydrogens H6N and H27N, respectively, whereas F3 is in bonding via two C−H···F (alkyl hydrogens H2B and H19B) and one N−H···F (amide hydrogen H2N) (Table 2). The observed C−H···F and N−H···F interaction distance and angles are within the range reported in the literature.[25a] The 14-point contacts of polyatomic and larger anion SiF_6^{2-} are analogous to the higher coordination known for the lanthanide metal complexes.[3]

Conclusion

The solid-state structural study of $\mathbf{L_1}$ shows that two of the three amide functional groups present in the ligand are in strong intramolecular hydrogen-bonding interactions which are further involved in aromatic $\pi\cdots\pi$ stacking, keeping the tripodal arms in close conformation. Protonation of the apical nitrogen favors intramolecular hydrogen-bonding interaction resulting in the interruption of intramolecular aromatic $\pi\cdots\pi$ stacking. Structural studies of the anion binding with the protonated triamide receptor show that not one of the guests is encapsulated inside the tren arm irrespective of size, shape, and charge of the anions. However, detailed structural investigation clearly demonstrates that the self-alignment, preorganization, and orientation of the multiple ligand moieties, depending upon the dimensionality of the incoming anionic guest, play a crucial role in making various molecular interactions in the binding of the anion outside the tripodal cavity. In all the complexes, aryl C−H···anion hydrogen bonds form mostly by the para hydrogen with respect to the NO_2 group and in some cases with the meta hydrogen, though calculations by Hay et al. on the $\mathbf{L_1}$ and NO_3^- complex reveal a NO_2 group para with respect to the hydrogen-bonding C−H groups, stabilizing the interaction with NO_3^- in the 1:1 complex.[13] This study also establishes bilayer structure formation in the solid state with a general tendency for protonation at the apical nitrogen and in the presence of an anionic guest in the triamide receptor, which was first reported by Bowman-James et al. for the $\mathbf{L_2}H^+NO_3^-$ complex.[16] Anion binding with other substituted tripodal ligands having electron donating groups at the aryl moiety is under investigation.

Acknowledgment. We thank Dr. P. K. Ghosh (Director, CSMCRI) for his constant support and encouragement. P.G. gratefully acknowledges the Department of Science and Technology, New Delhi, India (Grant No. SR/S1/IC-21/2002) for financial support. P.S.L. acknowledges CSIR, India, for a senior research fellowship.

Supporting Information Available: Six crystallographic files in CIF format of $\mathbf{L_1}$ and complexes **1**−**5** and additional crystallographic data including a table of hydrogen-bonding parameters, ORTEPs, and packing diagrams. This material is available free of charge via the Internet at http://pubs.acs.org.

IC052159O